Brazilian Journal of Geophysics 40 (2022), 4, 559-570
Brazilian Geophysical Society
ISSN 2764-8044
DOI: 10.22564/brjg.v40i4.2182

DETECTION OF DISCONTINUITIES IN POST-STACK 3D SEISMIC DATA USING INLINE AND CROSSLINE FILTERING

Gleidson Diniz Ferreira [1,2*] and Milton José Porsani [3,4]

[1]Petrobras, Rio de Janeiro, RJ, Brazil
[2]Universidade Federal da Bahia - UFBA, Curso de Pós-graduação em Geofísica, Salvador, BA, Brazil
[3]Universidade Federal da Bahia - UFBA, Institute of Geosciences, Salvador, BA, Brazil
[4] National Institute of Science and Technology of Petroleum Geophysics (INCT-GP/CNPq), Brazil

*Corresponding author email: gleidsondf@petrobras.com.br

ABSTRACT. The detection of seismic discontinuities in reflection seismology has gained prominence in recent years due to the increase in the quality of acquired seismic data, thus enabling a better prediction of structures such as faults and fractures and contributing to the improvement of the interpretation of conventional and non-conventional reservoirs. In view of the aforementioned facts, we present a three-step filtering methodology for detecting discontinuities in post-stack 3D seismic data: (i) firstly, a horizontal filtering (inline followed by crossline) is applied to attenuate most horizontal and sub-horizontal events (mainly associated with reflections in the layers), thus enhancing vertical and sub-vertical structures; (ii) secondly, the Hilbert transform is applied to each dimension of the volume to obtain the complex volume, and finally, (iii) a phase rotation is applied to each dimension of the amplitude volume. The final result is the highlighting of the fractures and flaws in the original volume. We illustrate the application of the new methodology in the prestack time migration of 3D seismic data of the Alto de Cabo Frio area, located between the Santos and Campos Basins. Numerical results demonstrate the aplicability of this methodology for detecting and mapping structural discontinuities in 3D seismic volumes, thus allowing for the delimitation of hydrocarbon reservoirs.

Keywords: faults; fractures; filtering; post-stack; interpretation

INTRODUCTION

Faults and fractures are structural features, generally easy identifiable in outcrops, of great importance in studies of petroleum systems, since they can act as permeability channels that connect source rock to reservoirs, performing as structural traps. The detection of faults and fractures has been highlighted in recent years due to the improvement in the quality of seismic data that allowed a better detection of these discontinuities in the exploration and production phases of oil and gas reservoirs.

For the oil and gas industry, discontinuity modeling is important for predicting the behavior of reservoirs in response to production (Ferreira et al., 2019), especially in relation to the detection of faults and fractures. This prediction can be made at the exploratory level, aiming to evaluate the recoverable reserves of an accumulation, in terms of porosities and mainly permeability, and it can also be made in the development, exploiting the reservoir in the best possible way.

Traditionally, faults and fractures are interpreted in sections and time slices of 3D seismic volumes as discontinuities in seismic amplitude or from time slices of a seismic coherence volume. Interactive tools have been developed to assist the interpreter in this process. Hale and Emanuel (2002) published the results of research focused on automatic meshing that could be applied to fault interpretation, and Pedersen et al. (2003) described a semi-automatic process for fault and fracture extraction using a volume of discontinuity in fracture modeling.

Seismic attributes based on detecting discontinuity of events provide useful tools for characterizing faults and fractures (Chopra and Marfurt, 2007). Conditioning the data increases the visual identification of faults and fractures in the seismic data and their attributes. Conditioned data can be processed to improve discontinuity features and therefore the attributes on this processed data will result in better extractions of faults and fracture geometry.

An example of conditioned data is the coherence cube calculated by measuring the similarity between features. Similar traces are mapped with high coherence coefficients, while discontinuities present low coherence. Regions of seismic traces cut by faults, for example, result in sharp discontinuities, generating a low coherence design along the fault planes (Chopra, 2002).

From this historical context on the importance of faults and fractures for the characterization of oil and gas reservoirs and the work already carried out to detect these discontinuities, we will propose a methodology for the detection of faults and fractures in the post-stack seismic data to assist in the quantitative geological interpretation and in the identification of possible accumulations of hydrocarbons. The presentation of this methodology is divided into three stages: In the first stage, an attenuation filter of horizontal and sub-horizontal events is applied, showing vertical and sub-vertical structures. In the second, a filter built from the Hilbert transform method is used for each of the three directions of the seismic volume that originates a volume of complex amplitude. In the last stage, a phase rotation is performed for each of the three directions of the complex volume, highlighting discontinuities such as faults and fractures. For a better detailing of this methodology, the theoretical foundation of the methods used will be presented first. In the next step, an application of this methodology will be presented in the PSTM 3D seismic data of the Alto de Cabo Frio area, located between the Santos and Campos Basins.

METHODS

Attenuation of horizontal and sub-horizontal reflections

In this first step, a single-channel filtering is performed in the inline direction followed by the crossline one, in order to attenuate sub-horizontal and horizontal events. Although for the attenuation of sub-horizontal events (dominantly reflections in the layers) different filters (derivative filters) can be used (Melo et al., 2009), after several tests, we chose to use the symmetric and simple filter, which subtracts the amplitude of the original data mean of the L samples in front of and behind its central position.

Let D represent the 3D seismic volume with *Ns, Nx, Ny* samples in the time, inline and crossline directions, respectively.

$$f(n) = \{f(-L), \cdots, f(-1), f(0), f(1), \cdots, f(L)\} = \left\{\frac{-1}{2L}, \cdots, \frac{-1}{2L}, 1, \frac{-1}{2L}, \cdots, \frac{-1}{2L}\right\}. \quad (1)$$

The filter $f(n)$, which has 2L+1 coefficients, is applied in cascade, initially in the inline direction,

$$D_x = f(n) * D(j) = \sum_{n=-L}^{L} f(n)D(j-n), \ (j = 1, ..., Nx) \quad (2)$$

and subsequently in the crossline direction,

$$D_{xy} = f(n) * D_x(k) = \sum_{n=-L}^{L} f(n)D_x(k-n), \ (k = 1, ..., Ny) \quad (3)$$

Where $*$ represents convolution.

Getting the amplitude of the complex 3D volume

Usually, the complex trace is obtained using the Hilbert Transform applied in the time direction, $H_t[D]$] (Claerbout, 1976; Taner *et al.*, 1979). In this section we will use the Hilbert transform, also in the inline, $H_x[D]$, and crossline, $H_y[D]$, directions. For this, we will use the quadrature operator, antisymmetric, or Hilbert filter.

As shown by Claerbout (1976), the series representing the Hilbert transform can be obtained with the Fast Fourier Transform method, taking the imaginary part of the inverse Fourier transform of the doubled frequency spectrum of the signal or doing the inverse Fourier transform over the frequency spectrum, multiplying the positive frequency components by i and the negative frequency components by $-i$. Another usual procedure is to convolve the sign with the quadrature operator, $h(n)$, given by the following expression:

$$h(n) = \frac{1}{2\pi}\int_{-\pi}^{\pi} \frac{-i\omega}{|\omega|} exp(-i\omega n)d\omega = \begin{cases} 0 & n \text{ even} \\ \dfrac{-2\pi}{n} & n \text{ odd} \end{cases} \quad (4)$$

As we use a fixed and small number of coefficients n (in this work we use the value of n = 3) in the operator $h(n)$, we need to apply a scale factor in the amplitudes that represent $H[D_t]$ to ensure that the energy of the signal and its Hilbert transform are equal. This scale factor that we call β is defined as:

$$\beta = \sqrt{\frac{\sum D_t^2}{\sum H[D_t]^2}}. \quad (5)$$

For simplicity of notation, we call the result of the first step (equation 3) $B = D_{xy}$, and we obtain the complex volumes in the time directions, inline and crossline, which we call directions $\{t, x, y\}$, respectively.

$$\begin{cases} B_t = B + iH_t[B], & (6a) \\ B_x = B + iH_x[B], & (6b) \\ B_y = B + iH_y[B]. & (6c) \end{cases}$$

where $H[\circ][B]$ represents the Hilbert transform of B in the direction $\circ$, obtained by convolving $h(n)$ (equation 4) with the volume traces B collected in the corresponding directions.

From the complex volumes, $\{B_t, B_x, B_y\}$, we get the volumes of the corresponding amplitude envelope (equation 7). The envelope is defined, according to Taner et al. (1979), as the total energy of the seismic trace, thus emphasizing the amplitude changes, and independent of the phase. In this work, the total energy of the seismic trace corresponds to the energy of the filtered data B plus the energy of the complex trace of the Hilbert transform of B in the directions t, x and y.

$$\begin{cases} A_t = \sqrt{B^2 + H_t[B]^2}, & (7a) \\ A_x = \sqrt{B^2 + H_x[B]^2}, & (7b) \\ A_y = \sqrt{B^2 + H_y[B]^2}. & (7c) \end{cases}$$

And so we get the average volume of the amplitudes,

$$\bar{A} = \sqrt{\frac{A_t^2 + A_x^2 + A_y^2}{3}}. \quad (8)$$

Enhancement of fractures and faults

In this third and last step of the process, we use again the Hilbert operator for phase rotation of the amplitude volume (equation 7) in the directions $\{t, x, y\}$. Through phase rotation (equation 9), we were able to organize the polarity and improve the enhancement of the filtered seismic signal. This resource is the same used in the Volume Amplitude Technique –tecVA– (Bulhões et al., 2005) which allows a better visualization of the seismic signal.

$$C = \frac{H_t[\bar{A}] + H_x[\bar{A}] + H_y[\bar{A}]}{3}. \quad (9)$$

Pseudo-code used in 3D volume filtering

Input:

L – Filter window size

$D(1 : Ns, 1 : Nx, 1 : Ny)$ – Original data

$f(n)$ – Inline and crossline reflection attenuation filter (equation 1)

$h(n)$ – Quadrature Operator (Hilbert filter) (equation 4)

Step 1 – Attenuating horizontal and sub-horizontal reflections

- Convolve f (n) with data in inline direction, (equation 2)
- Convolve f (n) with data in crossline direction, (equation 3)

Step 2 – Obtaining the amplitude of the complex 3D volume

- Convolve h(n) with data in time direction, (equation 6a)
- Convolve h(n) with data in inline direction, (equation 6b)
- Convolve h(n) with data in crossline direction, (equation 6c)
- Gets average volume from the amplitudes, (equation 8)

Step 3 – Highlighting fractures and flaws

- Gets Hilbert from the amplitude $\bar{A}$ in the directions $\{t, x, y\}$, and
- Obtains the average value, (equation 9)

NUMERICAL RESULTS

Methodology applied to the 3D PSTM data of the Alto de Cabo Frio area

The filtered data in step 2 were not used in the analysis of the results of this work because they present a similar result to the filtered data C calculated in step 3. In addition, the filtered data C highlight the structures present in the filtered data in step 2, allowing a better visualization.

In the first step of the methodology, a horizontal attenuation filter with $L = 1$ and three coefficients was used (the number of filter coefficients is 2L+1), as this parameterization presented better results than filters with $L > 1$. The attenuation filter was applied to the PSTM 3D seismic data from the Alto de Cabo Frio area (Figure 1) in cascade (as detailed in section **"Attenuation of horizontal and sub-horizontal reflections"**), that is, the filtering operator was applied

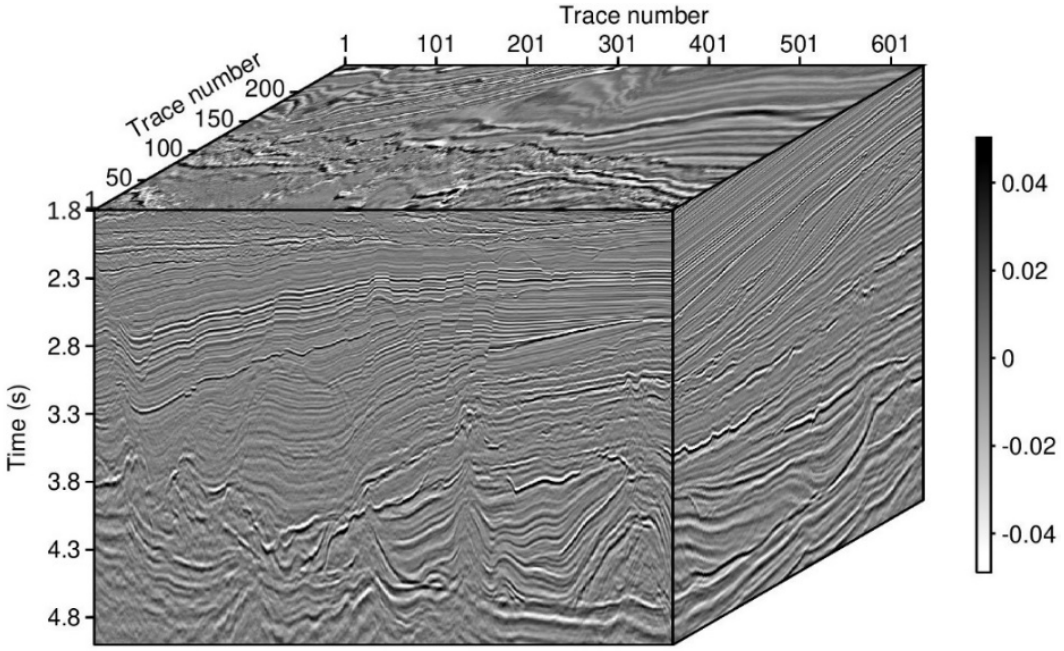

Figure 1: Original PSTM 3D seismic volume from the Alto de Cabo Frio area.

in the inline direction and then it was applied from the crossline direction, originating the filtered data B. With this, it was observed that in the filtered data B (Figure 2) there was an attenuation of the horizontal and sub-horizontal structures that highlighted the vertical and sub-vertical events.

The filtered data C (Figure 3) calculated from the application of the Hilbert filter in the last step of the methodology (section "Enhancement of fractures and faults") highlighted the vertical and sub-vertical structures, allowing a better visualization of faults and fractures.

Observing the average amplitude spectrum of the filtered data (Figure 4), it can be seen that the filtered data B decrease the amplitude of low frequencies, preserving and increasing the amplitude of high frequencies when compared to the original seismic data. This increase in contrast between low and high frequencies allows a better visualization of discontinuities such as faults and fractures. The filtered data C increase the content of low frequencies up to 5Hz, allowing the rise of the enhancement of vertical and sub-vertical structures.

Subsequently, to verify the effectiveness of the methodology, the filtered data C were used as input for the generation of geobodies that individualized faults and fractures in a 3D visualization software (dGB, 2022). This confirmed that the results were satisfactory, demonstrating a good continuity of faults and fractures throughout the seismic volume (Figure 5).

METHODOLOGY

Result in a Time Slice

Looking at the 2000ms time slice of the PSTM 3D seismic data from Alto de Cabo Frio area (Figure 6) and comparing it with the results presented by the filtered data B and C (Figures 7 and 8), it is noticed a better visualization of the strikes of some faults and fractures (directions L-W and NW-SE), mainly in the filtered data C, where these strikes are better highlighted. With this, it is concluded that the methodology used in this work is effective for visualizing faults and fractures in all directions studied (inline and crossline).

Result in a Seismic Line

Two seismic lines were extracted from the 3D PSTM seismic data of Alto de Cabo Frio area (Figures 9 and 12), each one cutting one of the two fault domains (L-W and NW-SE highlighted in Figures 6, 7 and 8) for better detailing of the analysis of the filtered data B and C when compared to the original seismic data (Figures 10 and 11 for the L-W fault domain and Figures 13 and 14 for the NW-SE fault domain). It was observed that, in the interval between 2000ms and 3000ms, there was a gain in the amplitude value of the filtered data B in relation to the vertical and sub-vertical structures and the attenuation of some horizontal and sub-horizontal structures when compared to the structures present in the original seismic data. The same happens with the filtered data C, where there is an enhancement of the amplitudes in the interval between 2000ms and 3000ms which corresponds to the fault zone present in the original seismic da

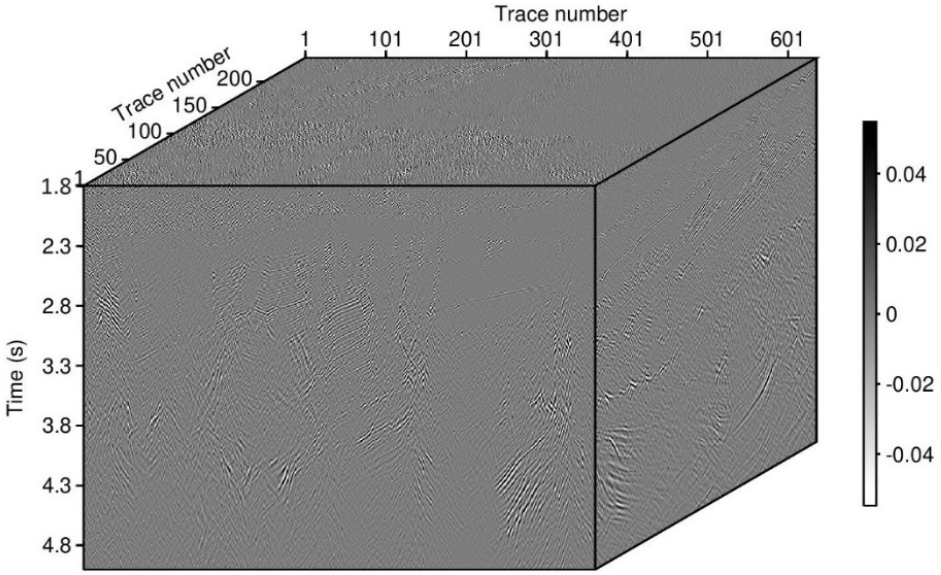

Figure 2: B-filtered data calculated from the application of the attenuation filter on the PSTM 3D seismic data of the Alto de Cabo Frio area.

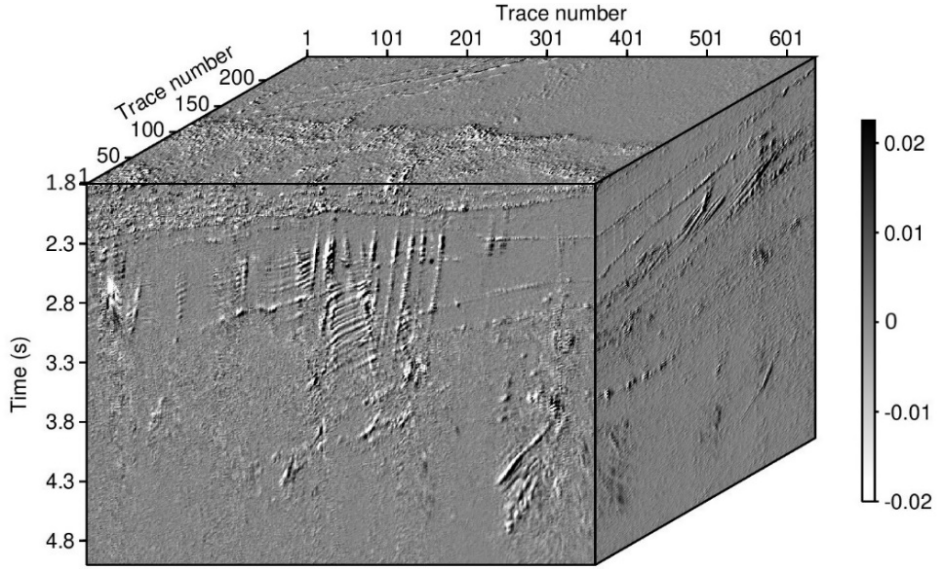

Figure 3: C-filtered data generated from the application of the Hilbert operator in the last step of the methodology.

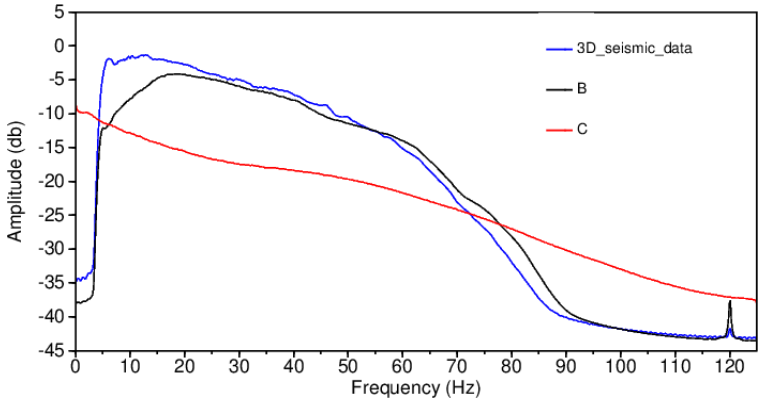

Figure 4: Average amplitude spectrum that compares the frequency range of the PSTM 3D seismic data from Alto de Cabo Frio area with the frequency range of the filtered data B and C.

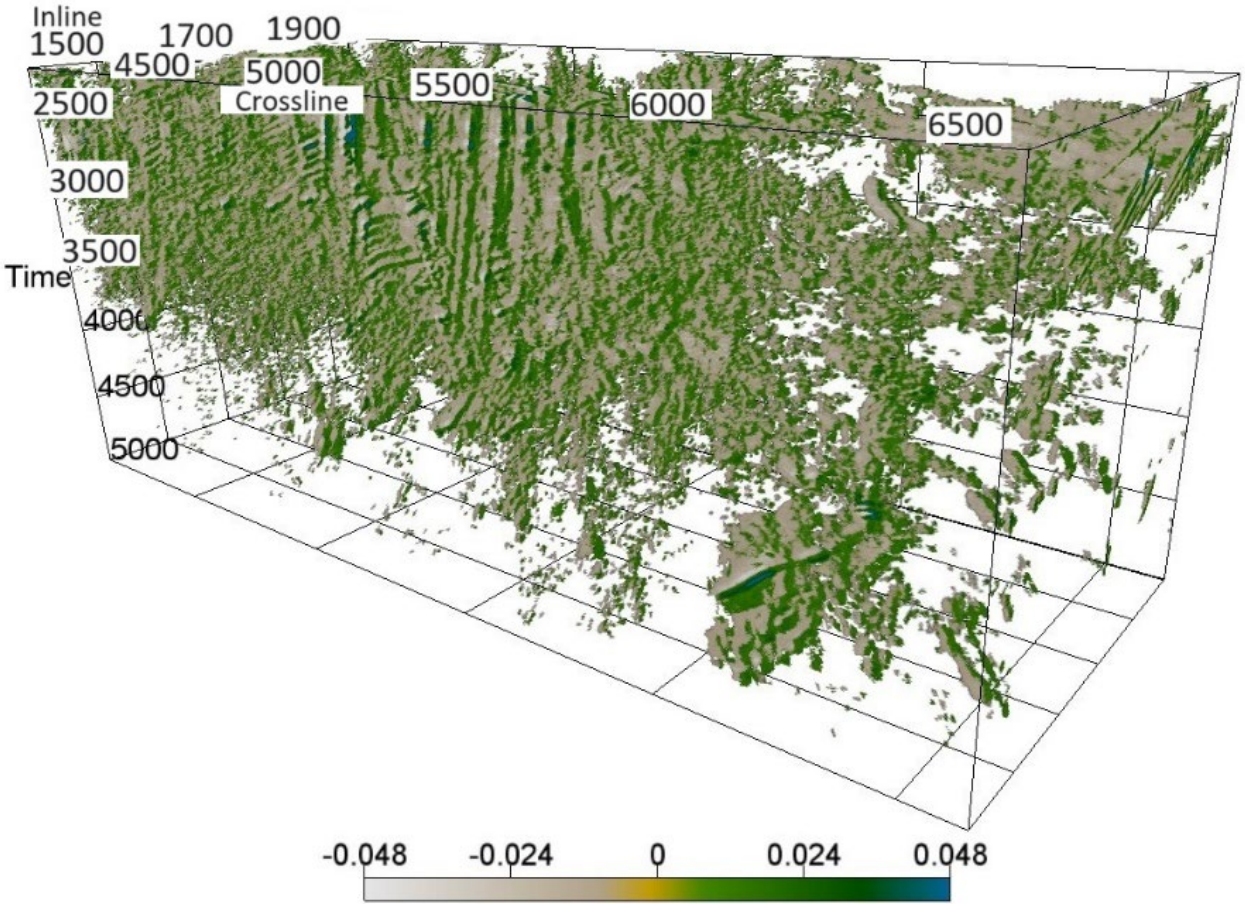

Figure 5: Geobodies created in OpendTect that individualize faults and fractures generated from the filtered data C.

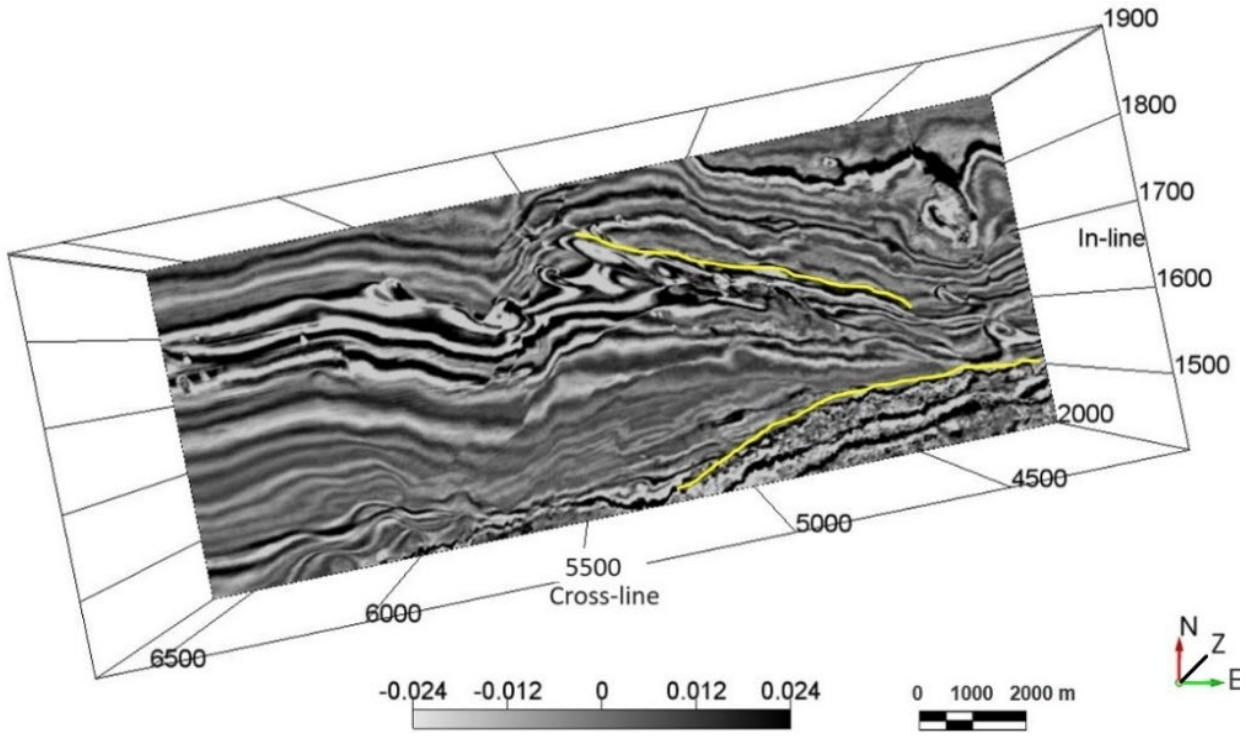

Figure 6: The 2000ms time slice of the original PSTM 3D seismic data from Alto de Cabo Frio area with the location of the L-W and NW-SE fault domains (highlighted in yellow).

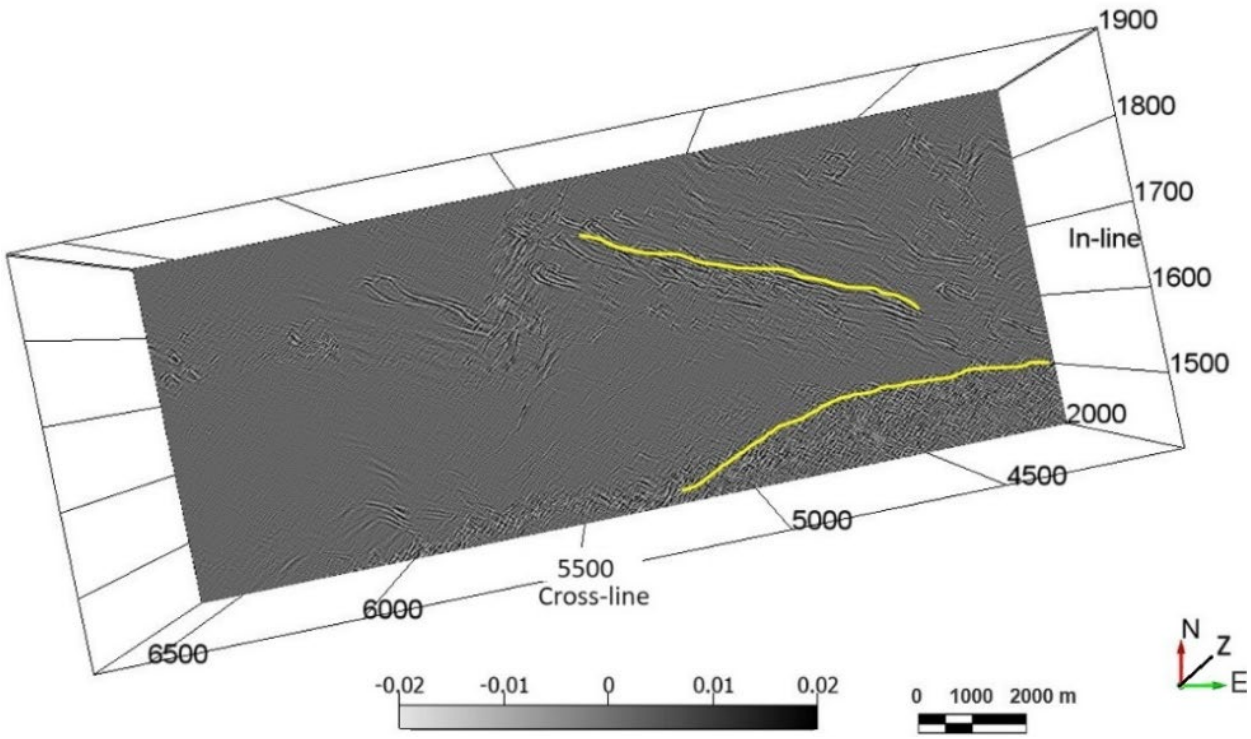

Figure 7: The 2000ms time slice of the filtered data B generated from the original PSTM 3D seismic data from Alto de Cabo Frio area with the location of the L-W and NW-SE fault domains (highlighted in yellow).

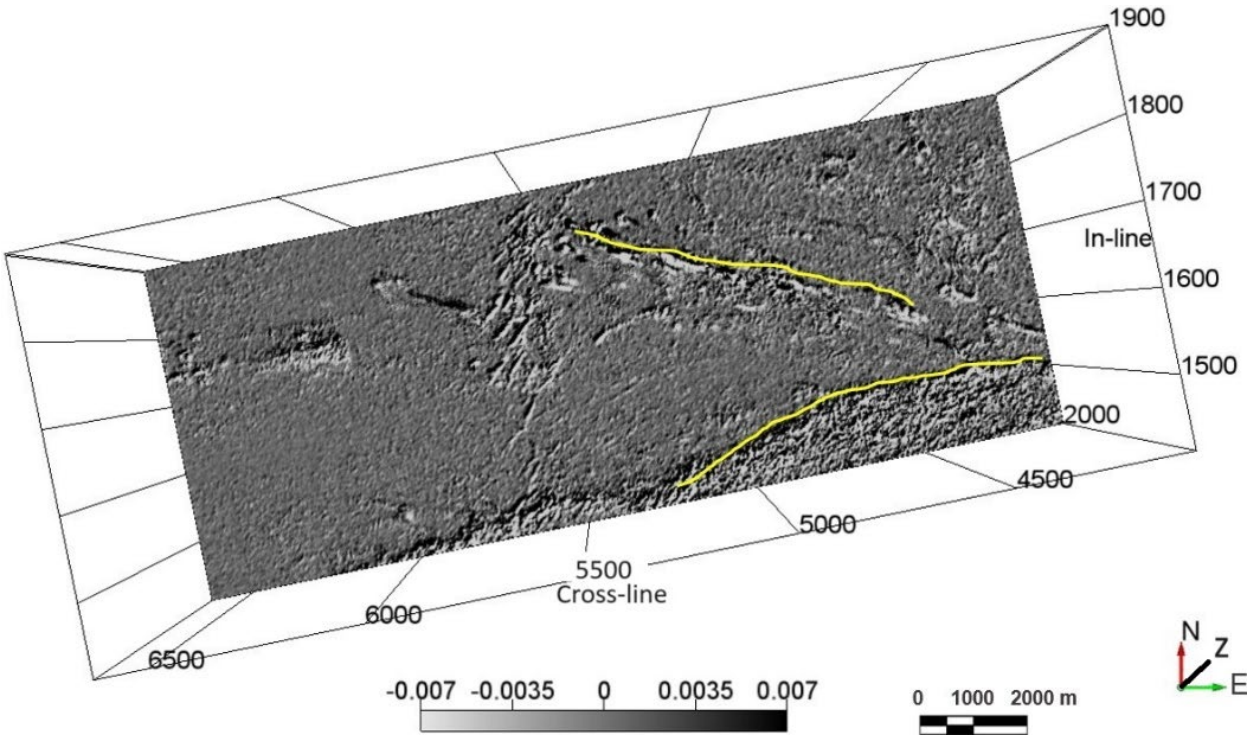

Figure 8: The 2000ms time slice of the filtered data C generated from the application of the Hilbert operator in the last step of the methodology with the location of the L-W and NW-SE fault domains (highlighted in yellow).

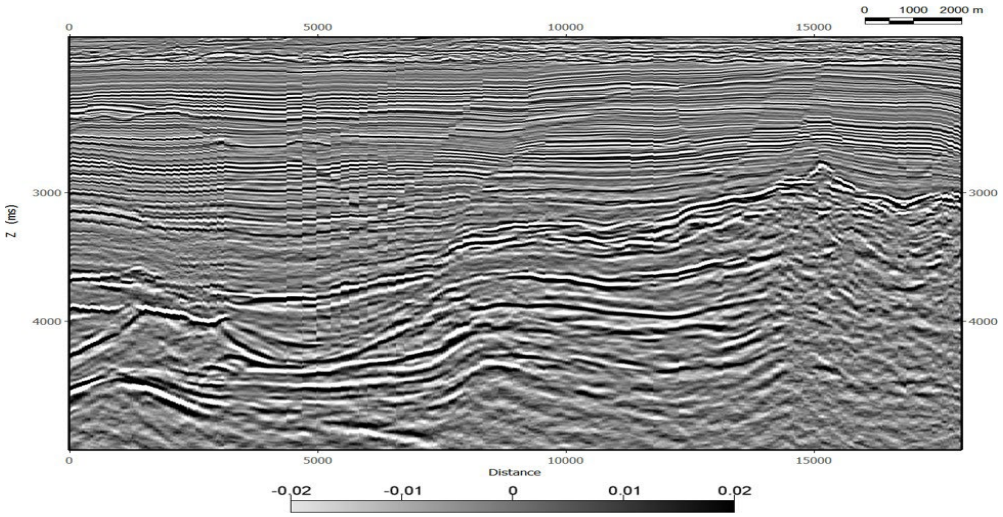

Figure 9: Original PSTM 3D seismic data from the Alto de Cabo Frio area (fault domain L-W).

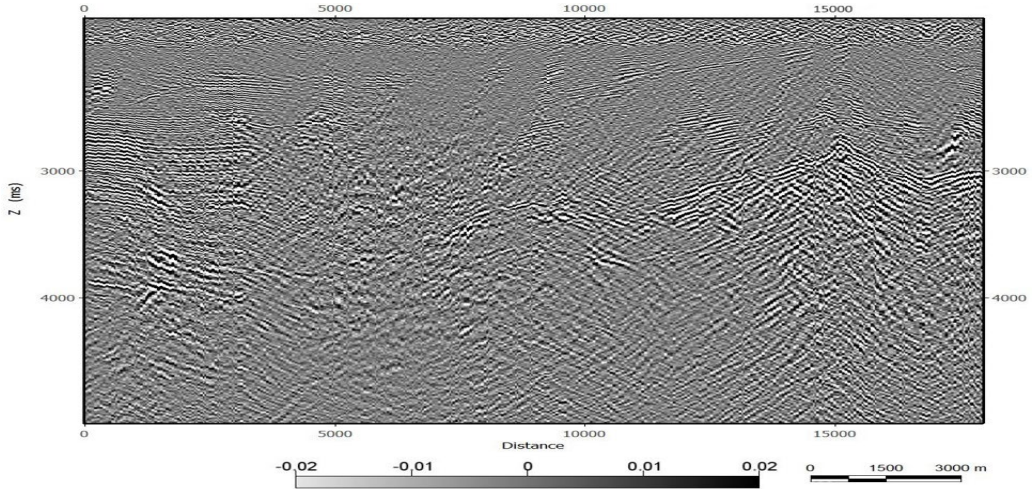

Figure 10: B-filtered data generated from the original PSTM 3D seismic data from Alto de Cabo Frio area (fault domain L-W).

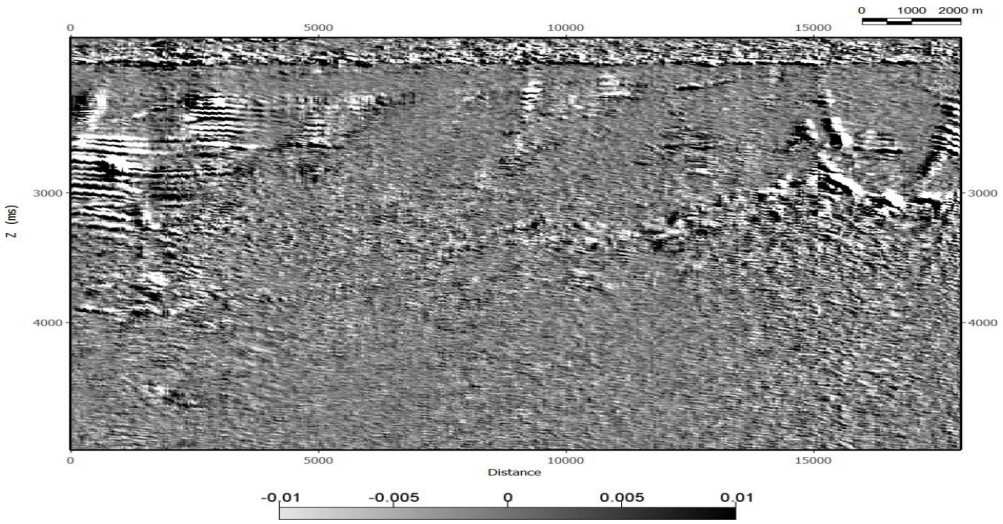

Figure 11: C-filtered data generated from the application of the Hilbert operator in the last step of the methodology (fault domain L-W).

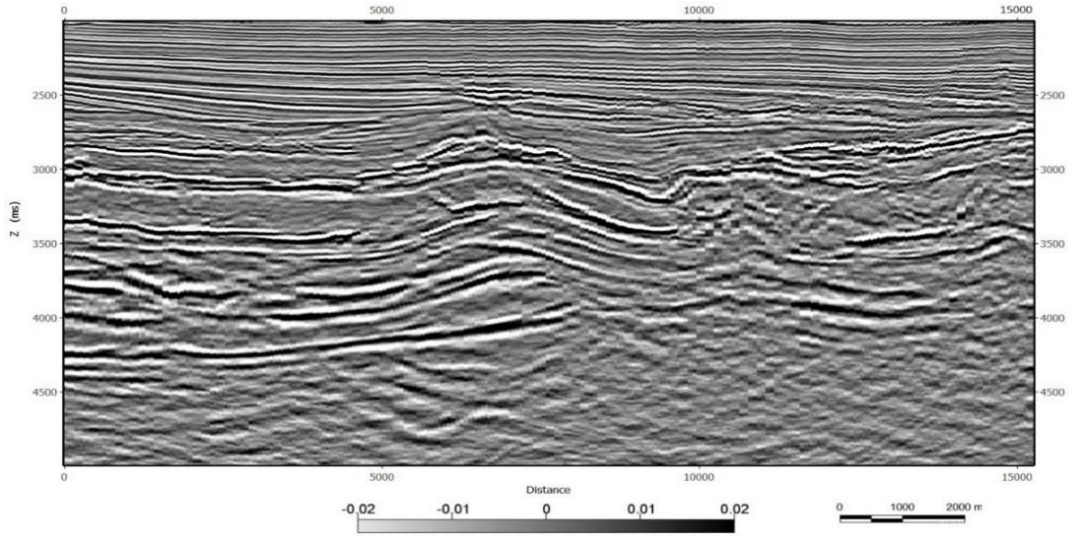

Figure 12: Original PSTM 3D seismic data from the Alto de Cabo Frio area (fault domain NW-SE).

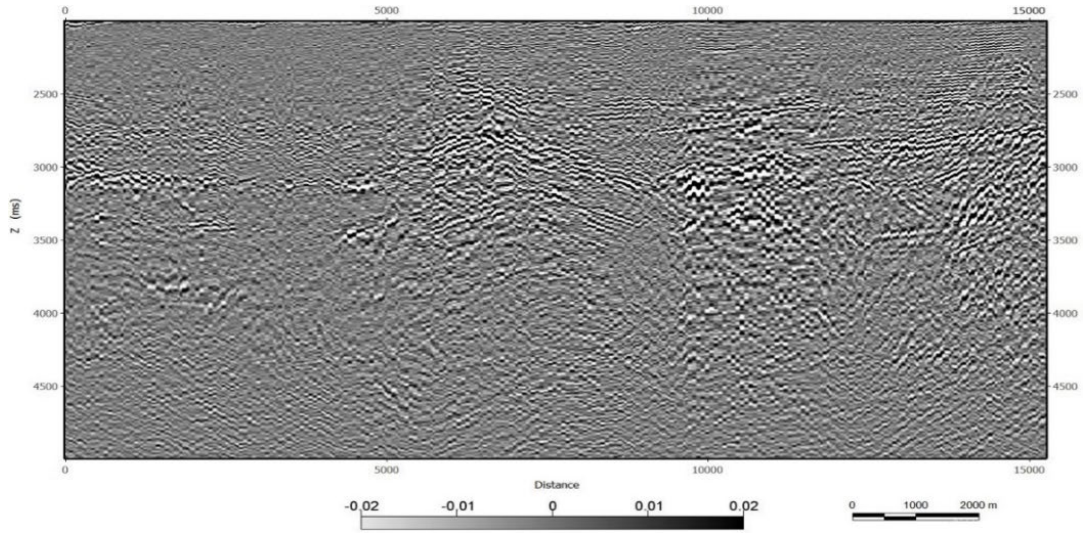

Figure 13: B-filtered data generated from the original PSTM 3D seismic data from Alto de Cabo Frio area (fault domain NW-SE).

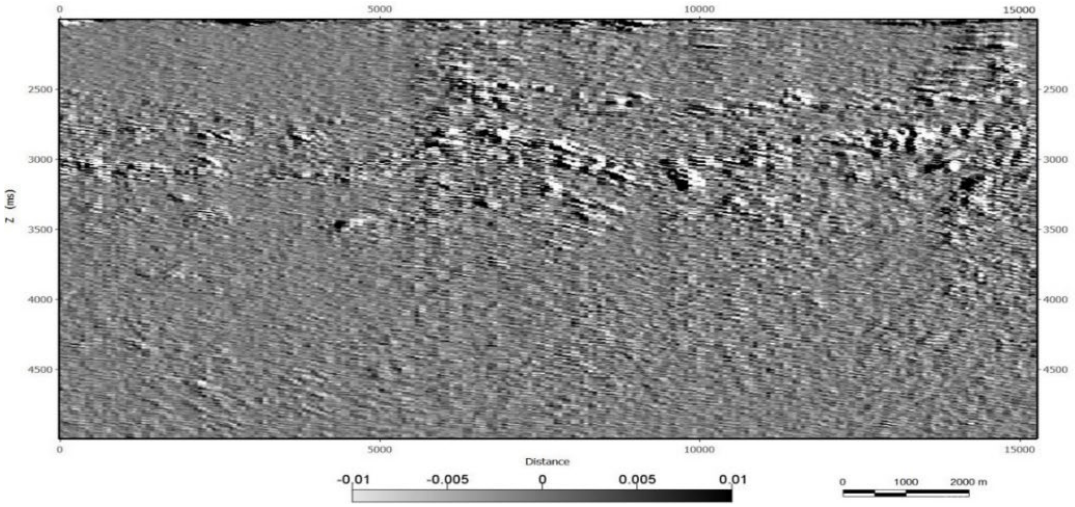

Figure 14: C-filtered data generated from the application of the Hilbert operator in the last step of the methodology (fault domain NW-SE).

DISCUSSION

The main similarity of the methodology presented in this work in relation to the works cited in the introduction section, such as the case of the coherence cube, is the provision of a tool capable of highlighting discontinuities; however, there is a big difference: the coherence cube uses a measure statistics of seismic traces to determine discontinuities, but despite providing good results, it highlights all events present in the seismic data (Figure 15), while the methodology presented in this work uses filters built to highlight discontinuities in certain directions, removing the influence of other events that are not important for the objective presented here, which is the enhancement of vertical and sub-vertical structures such as faults and fractures. This difference in relation to the traditional methods of detection of discontinuities ends up being the main advantage of the method used here.

Observing the average amplitude spectrum of the coherence cube (Figure 16) and comparing it with the spectra of the original PSTM 3D seismic data and the filtered data B and C, it can be seen an increase in the low and high frequencies, as well as in the data filtered C, however its curve presents a noise of sinusoidal aspect which is not observed in the other curves present in the graph of the average amplitude spectrum.

As was done in the filtered data C (section "Methodology applied to the 3D PSTM data of the Alto de Cabo Frio area"), we used the coherence cube as input for the generation of geobodies in a 3D visualization software (dGB, 2022). As seen in Figure 17, we were not able to clearly individualize structures such as faults and fractures, because the coherence cube also highlights events in other directions, unlike what is shown in Figure 5 with the geobodies created from the filtered data C.

Faults and fractures are tectonically distinct features. In the fracture, there is no displacement of the two sides of the structure, while the fault is characterized with a surface where there is a relative displacement between two sides of this structure. The algorithm implemented in the article cannot accurately differentiate what is fault or fracture. With this, the results obtained with the application of the algorithm only serve as an auxiliary in the exploratory interpretation. This allows the interpreter to define which are the areas where faults or fractures occur. The interpreter will analyze the results obtained and with this will verify, overlaying the original seismic, the discontinuities that make it possible to observe the tailings and will interpret them as faults, and where it is not possible to observe the tailings, the interpreter will be able to classify them as fractures.

As the methodology presented in this work was built only for the detection of vertical and sub-vertical structures, this fact ends up as its main limitation; however, the filtering direction can be redefined to detect seismic events in other directions, if the intention to change the purpose of discontinuity detection.

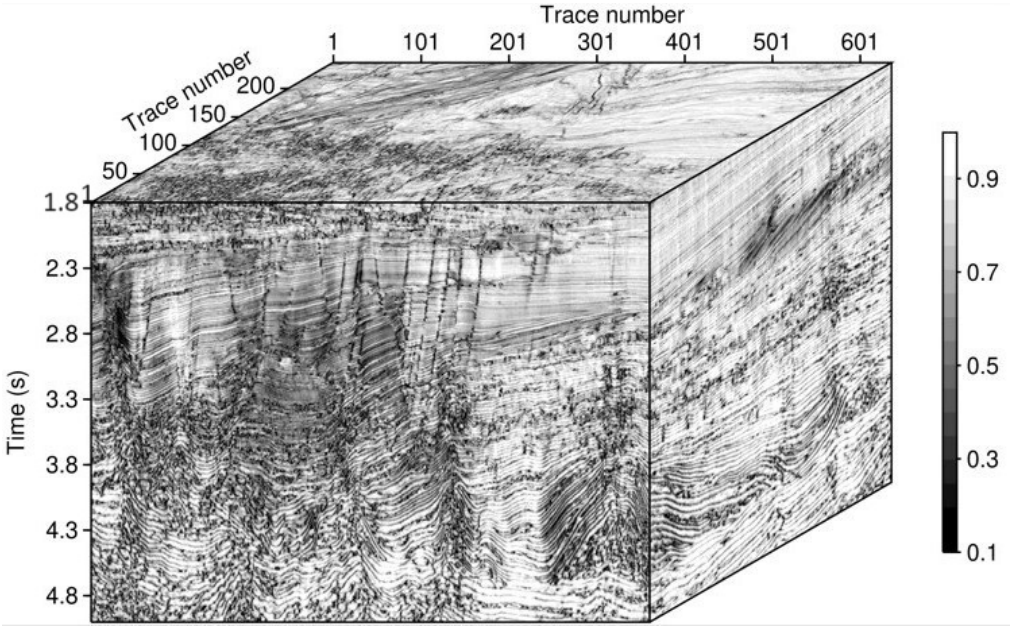

Figure 15: Coherence cube created in OpendTect (dGB, 2022) from the original PSTM 3D seismic volume of the Alto de Cabo Frio area. It is observed that structures such as faults and fractures are highlighted, but the events in other directions are also enhanced.

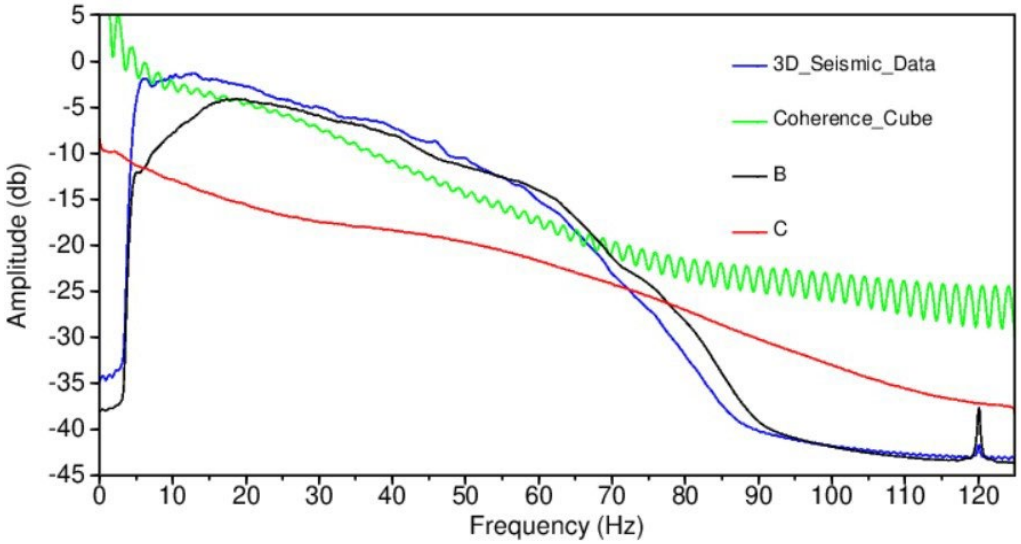

Figure 16: Average amplitude spectrum comparing the frequency range of the PSTM 3D seismic data from Alto de Cabo Frio area with the frequency range of the coherence cube and filtered data B and C.

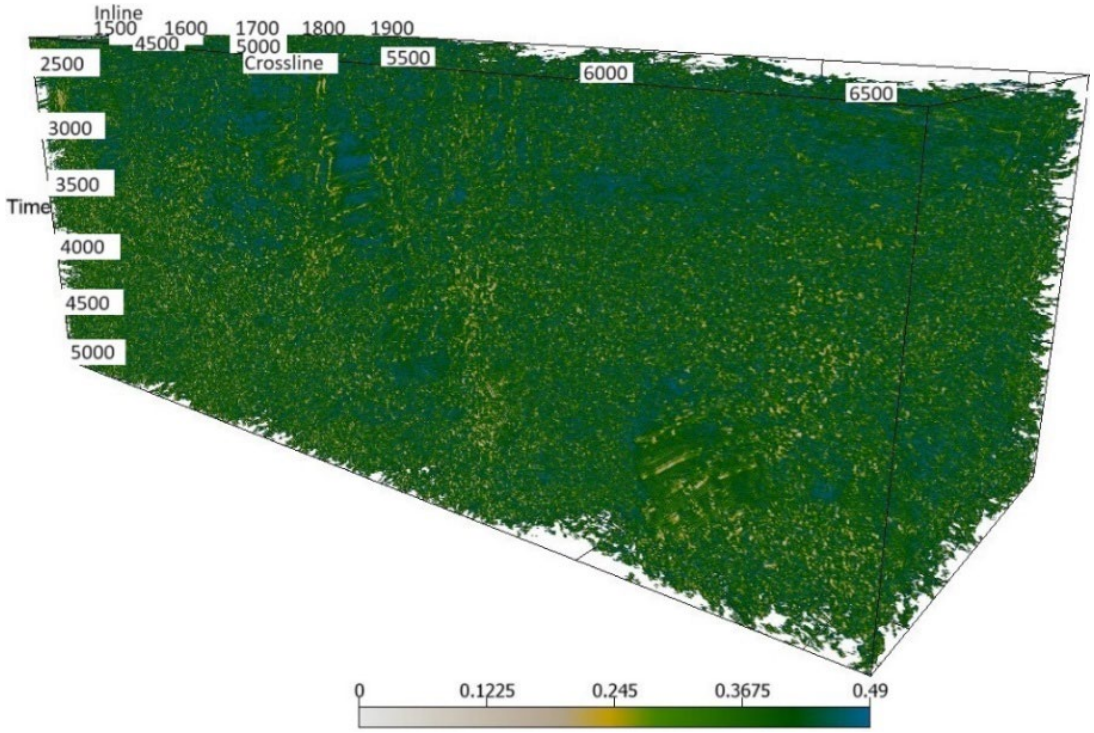

Figure 17: Geobodies created in OpendTect from the coherence cube.

CONCLUSIONS

The detection of discontinuities using filtering methods oriented according to certain directions (horizontal or vertical, depending on the proposed objective) in the post-stack seismic data, such as those presented in this work, provides important tools for the characterization of faults and fractures. The precision and quality of these filtering methods are directly proportional to the signal/noise ratio of the seismic data, that is, the higher this ratio, the better the quality of the filtered data generated. The results presented with the application of the attenuation filter of horizontal and sub-horizontal structures improved the visual identification of vertical and sub-vertical structures in the seismic data, which benefits the exploratory interpretation. In addition, the filtered data C were able to satisfactorily highlight some discontinuities present such as faults and fractures, thus facilitating the delimitation of hydrocarbon reservoirs.

REFERENCES

Bulhões, E.M. and Amorim, W.N., 2005, Princípio da SismoCamada Elementar e sua aplicação à Técnica Volume de Amplitudes (tecVA): 9th International Congress of the Brazilian Geophysical Society. Expanded Abstracts. Salvador, BA, Brazil. Sociedade Brasileira de Geofísica, doi: 10.1190/sbgf2005-275.

Chopra, S. Coherence Cube and Beyond., 2002, First Break, **20**, 1. doi: 10.1046/j.1365-2397.2002.00225.x.

Chopra, S. and Marfurt, K.J., 2007, Seismic Attributes for Fault/Fracture Characterization: SEG Annual Meeting. San Antonio, Texas. Paper Number: SEG-2007-1520. doi: 10.1190/1.2792785.

Claerbout, J.F., 1976, Fundamentals of Geophysical Data Processing: With Applications to Petroleum Prospecting. McGraw-Hill, New York. 274 pp.

dGB Beheer B.V., 2022, OpendTect User Documentation - 6.6. dGB Earth Sciences. Netherlands.

Ferreira, G.D., Bulhões, F.C., Santos, R.A., Carvalho, J.G., Tanaka, A., and Lira, J.E.M., 2019, Construction of a fracture model from the PSDM seismic in the Rio Neuquén Basin: 16th International Congress of the Brazilian Geophysical Society, 2019, Expanded Abstracts. Rio de Janeiro, RJ, Brazil. Sociedade Brasileira de Geofísica, doi: 10.22564/16cisbgf2019.094.

Hale, D. and Emanuel, J., 2002, Atomic meshing of seismic images: 72nd Annual International Meeting, SEG, Expanded Abstracts, Salt Lake City, Utah. 2126–2129, doi: 10.1190/1.1817124.

Melo, P.E.M., Porsani, M.J., and Silva, M.G., 2009, Ground-roll attenuation using a 2D time derivate filter. Geophysical Prospecting, **57**, 343–353, doi: 10.1111/j.1365-2478.2008.00740.x.

Pedersen, S., Skov, T., Hetlelid A., Fayemendy P., Randen, T., and Sonneland, L., 2003, New paradigm of fault interpretation, presented at the 73rd Annual International Meeting, SEG, Expanded Abstracts, Dallas, Texas. Paper Number: SEG-2003-0350. doi: 10.1190/1.1817918.

Taner, M.T., Koehler, F., and Sheriff, R.E., 1979, Complex seismic trace analysis: Geophysics, **44**, 1041–1063, doi: 10.1190/1.1440994.

Ferreira, G.D: conceptualization, development, figure generation, methodology results, result discussion, manuscript final version**; Porsani, M.P:** conceptualization, theory exposition, result discussion, manuscript final version.

Received on April 29, 2022 / Accepted on January 11, 2023